# Elastic Moduli of $Ge_xSe_{100-x}$ ($x \leq 10$) Glasses in the Transition Range: Implications for Elastic Models of Viscous Flow

**Hao Chen, Sabyasachi Sen***

*Department of Materials Science & Engineering, University of California at Davis,*
*Davis, CA 95616, USA*

**Corresponding Author: Sabyasachi Sen (email: sbsen@ucdavis.edu)*

## Abstract

The elastic moduli of $Ge_xSe_{100-x}$ ($0 \leq x \leq 10$) glasses and deeply supercooled liquids are determined across the glass transition between ambient temperature and 1.16 $T_g$ using resonant ultrasound spectroscopy. The temperature dependence of the high-frequency shear modulus $G_\infty(T)$ at T > $T_g$ is found to be consistent with the predictions of the elastic models of viscous flow that consider the energy barrier to the structural rearrangement associated with an elementary flow event to be governed by $G_\infty(T)$. A strong correlation between the fragility indices of these liquids and $|\frac{\partial G_\infty}{\partial T}|$ at T > $T_g$ indicates a clear connection between their entropic and elastic properties. Finally, the rise in the Poisson's ratio of these liquids with temperature is argued to be a consequence of the composition dependence of $\frac{\partial G_\infty}{\partial T}$, as the temperature derivative of their bulk modulus is an order of magnitude lower than $\frac{\partial G_\infty}{\partial T}$ at T > $T_g$.

## 1. Introduction

The mechanistic understanding of the temperature dependence of kinetic slowdown and eventual glass transition of glass-forming liquids (GFL) at an atomic level, remains an unresolved and controversial topic in condensed matter physics. A wide range of theoretical models have been proposed in the literature to explain the remarkable rise in viscosity $\eta$ of a GFL upon cooling, often by more than 12 orders of magnitude within a relatively narrow temperature range, along with a concomitant increase in its activation energy [1,2]. The key ingredients of these theoretical models range from the temperature dependence of the free volume to that of the configurational entropy or of the shear modulus of the GFLs [1–6]. Moreover, equivalence between some of these models has also been hypothesized, based on a deeper physical connection between the entropic and elastic properties [7] . The Maxwell relation $\eta = G_\infty \tau$ connects the viscosity $\eta$ of a GFL with its shear relaxation timescale $\tau$, with $G_\infty$ being the high-frequency shear modulus of the liquid [1,2,8]. Since as a multiplicative factor $G_\infty$ depends weakly on temperature, the Maxwell relation implies a similar temperature dependence of $\eta$ and $\tau$.

The configurational entropy model of Adam and Gibbs hypothesized that viscous flow of a GFL involves cooperative structural rearrangement and the continuous increase in the activation energy of this process upon cooling was related to the increasing size $z$ of these cooperatively rearranging regions such that $\tau \propto exp\left(\frac{z\Delta g}{RT}\right)$ [3]. Here $\Delta g$ is the average temperature-independent energy barrier associated with the cooperative rearrangement of elementary structural units. The configurational entropy $S_c(T)$ of a GFL is expected to decrease on cooling due to the increase in $z$ such that $z \sim 1/S_c$ and thus $\tau$ can be written as:

$$\tau = \tau_0 \, exp\left(\frac{\Delta G}{TS_c}\right) \qquad (1)$$

where $\tau_0$ is a constant and $\Delta G$ is the activation enthalpy of shear relaxation and viscous flow. The $\Delta g$ or $\Delta G$ is considered to be independent of temperature in the Adam-Gibbs formalism and thus $S_c(T)$ is solely responsible for the temperature dependence of $\tau$ or $\eta$. In contrast, the elastic models of viscous flow [2,5,9,10] note that the energy barrier $\Delta G$ to structural rearrangement can be directly linked to the shear modulus $G_\infty$, as the elementary flow event of a structural unit requires creation of excess volume via a local deformation of the surrounding, which results in a decrease in density. Therefore, even a weak temperature dependence of $G_\infty$ could render $\tau$ strongly temperature dependent due to the latter's exponential dependence on $\Delta G$. Dyre and coworkers have shown that in this scenario [2,10]:

$$\tau = \tau_0 exp\left[\frac{G_\infty(T)V_c}{k_B T}\right] \qquad (2)$$

where $V_c$ is a characteristic volume of the rearrangement region that is considered in its original formulation to be independent of temperature. An important prediction of Eq. 2 is that log $\tau(T)$ or log $\eta(T)$ is a linear function of $G_\infty/T$ and should collapse on a universal trend if $G_\infty/T$ is suitably normalized and $V_c$ can be considered a system-independent constant.

It may be noted here that in a previous study one of us hypothesized a direct connection between $S_c$ and $G_\infty$ by considering contributions to $G_\infty$ from (i) uniform deformation as well as from (ii) structural rearrangement in amorphous materials, and by relating the latter contribution to $S_c$ [7]. It was shown that as the $G_\infty(T)$ of a supercooled liquid decreases with temperature the $S_c(T)$ of the liquid is expected to increase. Considering that the fragility index $m$ of a GFL, which is a measure of the departure of its viscosity from an Arrhenius behavior and is defined as [11]:

$$m = \left.\frac{d\log_{10}\tau}{d(T_g/T)}\right|_{T=T_g} \qquad (3)$$

with $T_g$ being the calorimetric glass transition temperature, a combination of Eqs. (1) and (3) implies that $m \propto \frac{dS_{conf}}{dT}|_{T \to Tg}$ [12]. Therefore, this model would suggest a correlated variation between $m$ and $|\frac{\partial G_\infty}{\partial T}|$ at T > $T_g$. On the other hand, Rouxel [9] has argued that the energy barrier to viscous flow being proportional to $G_\infty$, the activation entropy of viscous flow is directly related to $dG_\infty/dT$. Within this thermodynamic framework, when one considers the empirical negative linear correlation between $m$ and the stretching exponent β of the non-exponential shear relaxation that is ubiquitously characteristic of the deeply supercooled state of GFLs [13], Rouxel's model predicts $m \propto -\left(\frac{1}{1-\chi}\right)$ , where $\chi = \frac{T}{G_\infty}\frac{\partial G_\infty}{\partial T}|_{T=T_g}$. However, Nemilov [5] has pointed out that experimental observation of any correlation between viscous and elastic properties of GFLs may be contingent upon comparison within systems with related structural and bonding characteristics.

Therefore, an atomistic understanding of the elastic model and a rigorous experimental validation of its predictions require the determination of $G_\infty(T)$ and $\eta(T)$ at temperatures near the glass transition range for supercooled GFLs with systematic structural evolution and with a wide range of fragility indices, which remain scarce in the literature. Here we present such data and test the predictions of the elastic model in the case of chalcogenide GFLs in the binary system $Ge_xSe_{100-x}$ ($0 \le x \le 10$) with structures ranging from 1D chains to substantially connected networks with average coordination numbers ranging between 2.0 and 2.2 and $m$ ranging between 45 and 80.

## 2. Experimental

### *2.1. Sample preparation and physical characterization*

The $Ge_xSe_{100-x}$ (x = 0, 2, 5, 7.5, 10) glasses were synthesized from the constituent elements (≥99.999% purity, metal basis) that were melted in evacuated ($10^{-6}$ Torr) fused silica ampoules in a rocking furnace at 800 K. The melts were quenched to obtain glass by dipping the ampoules in water to form glasses. The $T_g$ of these glasses was determined using differential scanning calorimetry (Mettler Toledo DSC1). Samples of mass ~15-25 mg were taken in hermetically sealed Al pans and heated at a rate of 10K/min in a flowing nitrogen environment to $T_g$+20K to remove thermal history. The $T_g$ was taken as the onset of the endothermic glass transition signal while heating the sample at 10 K/min subsequent to cooling at the same rate from $T_g$+20K after the first heating cycle. $T_g$ was determined to within ± 2 °C as the onset of the glass transition endotherm. Density of these glasses was measured using a gas expansion pycnometer (Micromeritics AccuPyc II 1340) at 20°C using helium (6N purity) as the displacement gas. For each measurement, approximately 0.5 g of glass sample was loaded into a 1 $cm^3$ cup. All density values are taken as averages of 10 consecutive measurements of each sample.

### *2.2. Elastic modulus measurement*

The various elastic moduli of these $Ge_xSe_{100-x}$ glasses were determined using resonant ultrasound spectroscopy (RUS). Measurements were carried out using a spectrometer (ACE-RUS008) designed at the Los Alamos National Laboratory [14]. The free-body mechanical resonances of ~ mm sized samples are used in RUS to determine their complete elastic modulus matrix [14,15]. Details on the experimental setup and data analysis for RUS can be found in the literature [14,15]. The glass samples were cut into a rectangular parallelopiped geometry (~ 7mm x 5mm x 3mm) and all surfaces of these samples were polished flat and parallel. The as-prepared samples were mounted on opposing corners between two piezoelectric transducers. All measurements were carried out in a flowing nitrogen environment. The gas was heated with a resistive heater for measurements at temperatures above the ambient to up to 375 K. The sample temperature was measured using a Si diode temperature sensor mounted within a few mm from the sample. The RUS measurements involve the generation of an elastic wave of constant amplitude and varying sweeping frequency by the drive transducer and the acquisition of a resonant frequency spectrum with the pickup transducer. For each $Ge_xSe_{100-x}$ glass such spectra were acquired in the frequency range between 50 kHz and 400 kHz (Fig. 1) as a function of temperature. The location of the resonances in these spectra are subsequently identified for a free-surface rigid solid with the geometry and density corresponding to the sample (Fig. 1), using the Lagrangian minimization code developed at the Los Alamos National Laboratory [14,15]. The code then uses the mechanical resonances of the solid thus obtained, to compute its elastic properties using an iterative inversion procedure, where forward computations on a varying elastic tensor are performed until the calculated set of resonances agree with the measured ones within some predefined threshold [14].

## 3. Results and Discussion

The temperature dependence of $G_\infty(T)$ of all glasses at $T< T_g$ and in the deeply supercooled regime in the temperature range $T_g < T \leq 1.16\ T_g$, are shown in Fig. 2. As expected, and consistent with previous studies on a wide variety of glasses and supercooled GFLs, $G_\infty$ decreases monotonically and approximately linearly with increasing temperature over both temperature ranges [9,16]. Moreover, it is clear that $G_\infty$ decreases more rapidly in the supercooled liquid state above $T_g$ compared to that in the glassy state at temperatures below $T_g$. A glass transition temperature can thus be defined as the onset temperature for the change in $|\frac{\partial G_\infty}{\partial T}|$ in Fig. 2. This onset temperature is remarkably consistent with the calorimetric $T_g$ of these compositions measured using DSC, although the former is found to be systematically lower by a few degrees

(Fig. 3). Previous studies in the literature reported a similar observation, where the $G_\infty(T)$ of a diverse range of GFLs were measured at significantly different frequencies using a wide variety of experimental techniques [9]. Here we hypothesize that the observed difference in $T_g$ is likely indicative of the calorimetric (enthalpic) and "elastic" glass transition being controlled by the same structural rearrangement process where the two methods probe the process at different length scales and thus represent different parts of the associated relaxation time distribution [17]. In this scenario the elastic glass transition is expected to probe a smaller length scale and thus has a lower onset temperature on heating compared to the enthalpic glass transition.

The relationship between the thermal expansion coefficient $\alpha$, the Grüneisen parameter $\gamma$ of the transverse sounds waves and the elastic modulus $E$ of a solid can be expressed as: $\alpha = \frac{\gamma \rho C_v}{E}$, where $\rho$ is the density of the solid and $C_v$ is its heat capacity at constant volume [18]. As the various elastic moduli of a solid are related to one another, and $\alpha$, $\gamma$ and $C_v$ of a glass can be treated as constants, at least over a limited temperature range below the glass transition, the $|\frac{\partial G_\infty}{\partial T}|$ of any glass at $T < T_g$ in Fig. 2 is expected to be primarily controlled by $d\rho/dT$ i.e. by its volume thermal expansion coefficient. This expectation is borne out in Fig. 4 where the $|\frac{\partial G_\infty}{\partial T}|$ of the chalcogenide glasses at $T < T_g$ is indeed observed to be a monotonic function of the volume expansion coefficient.

In contrast to the relatively slow variation of $G_\infty$ with temperature at $T < T_g$, the $|\frac{\partial G_\infty}{\partial T}|$ increases by nearly an order of magnitude in the supercooled liquid state. Such a large increase in $|\frac{\partial G_\infty}{\partial T}|$ cannot be explained by the corresponding increase in $\alpha$ of these liquids by only a factor of 2-3 across the glass transition [19]. Therefore, the sharp increase in $|\frac{\partial G_\infty}{\partial T}|$ must be related to the onset of structural rearrangement and relaxation in these supercooled liquids above $T_g$. The temperature dependence of the viscosity of these liquids are shown in Fig. 5. It is clear that, consistent with the prediction of the elastic shoving model [2,10], the logarithm of the viscosity of these liquids tends to collapse on a linear trend when plotted as a function of $G_\infty$/T, despite the large spread of viscosity as a function of $T_g$/T owing to the wide range of the fragility index. Moreover, a linear least-squares fit to the collapsed data yields a reasonable viscosity of ~ $10^{-3}$ Pa.s at infinite temperature [20]. The $|\frac{\partial G_\infty}{\partial T}|$ at T > $T_g$ for these GFLs shows a systematic and monotonic increase with $m$ (Fig. 6a) that may be indicative of a direct connection between $S_c$ and $G_\infty$ [7]. On the other hand, as noted earlier, Rouxel's model [9] based on equating activation entropy of viscous flow to $\frac{\partial G_\infty}{\partial T}$ predicts $m \propto -\left(\frac{1}{1-\chi}\right)$. As shown in Fig. 6b, this prediction is also borne out by the present data with $m$ displaying a nearly linear negative correlation with $\left(\frac{1}{1-\chi}\right)$. Further systematic studies on other glass-forming systems are therefore required to distinguish between these two models, though the existence of a connection between the entropic and elastic properties in GFLs appear to be clear.

It may be noted here that although the present study, to the best of our knowledge, reports the $G_\infty(T)$ of $Ge_xSe_{100-x}$ glasses and GFLs with $x \leq 10$ for the first time, that of amorphous and supercooled Se was reported in a previous study by Gueguen et al. [16]. In this study the authors used a resonant frequency technique, and the shear modulus was measured on plate-like samples in torsion mode over a frequency range that was significantly lower (1-10 kHz) than that used (50-400 kHz) in the present study. This study reports significantly higher slopes $\frac{\partial G_\infty}{\partial T}$ both below and above $T_g$ for Se (~ −0.022 and −0.15 GPa.K$^{-1}$, respectively) compared to those determined in the present study (~ −0.0054 ±0.0005 and −0.067 ±0.003 GPa.K$^{-1}$, respectively). The origin of this large discrepancy remains unclear at this point but may be suggestive of the possibility that the effects of relaxation on the modulus cannot be completely ignored even at frequencies that are substantially higher than the average structural relaxation time at these temperatures, since the distribution of relaxation times can be extremely broad, especially in fragile liquids such as Se, near the glass transition. This issue needs to be further investigated in future by comparing elastic moduli measurements on GFLs across glass transition using a variety of techniques that cover a wide frequency range from kHz (e.g. resonant techniques) to GHz (e.g. Brillouin spectroscopy).

Finally, the temperature dependent evolution of the Poisson's ratio of the $Ge_xSe_{100-x}$ GFLs is shown in Fig. 7. The Poisson's ratio ν increases rapidly with increasing temperature above $T_g$ and $\frac{\partial \nu}{\partial T}$ appears to be strongly correlated to $\frac{\partial G_\infty}{\partial T}$ (Fig. 7). This increase in ν is consistent with the fact that in general, compared to glasses, liquids are weakly compressible, and stress in the latter primarily results in shape change more than volume change [21]. Consequently, liquids are characterized by relatively higher bulk:shear modulus ratio $B_\infty/G_\infty$ and ν (approaching its limiting value of 0.5) compared their glassy counterparts. A number of previous studies reported similar observation in a variety of GFLs and ascribed it to a progressive structural disintegration of the liquid with increasing temperature [9,16,21]. This hypothesis has its origin in the negative correlation between ν and structural connectivity observed in network glasses. Examples of such temperature-induced structural disintegration were speculated to be (i) fragmentation of chains in the case of selenium or (ii) conversion of boroxol rings in $B_2O_3$ to chains of $BO_3$ triangles and eventually to isolated $BO_3$ molecular units[9] . However, it may be noted that such structural disintegration of network liquids, although perhaps appealing, may not be physically sensible unless it is considered to be rather localized, rare and only transient events. For example, conversion of a $B_2O_3$ network into isolated $BO_3$ molecules would have charge balance and stoichiometry problems as the B:O ratio would increase from 1:1.5 in the former to 1:3 in the latter and the $[BO_3]^{-3}$ units will be highly negatively charged. Similarly, fragmentation of Se chains would result in a significant fraction of singly-coordinated Se atoms, for which experimental proof remains lacking in the literature. It is important to note here that the bulk modulus $B_\infty$ of these $Ge_xSe_{1-x}$ GFLs also decrease with temperature above $T_g$, albeit at a rate that is an order of magnitude lower than that displayed by $G_\infty$ (Fig. 8), and consequently, the temperature dependence of the ratio $\frac{B_\infty}{G_\infty} = \frac{2}{3}\frac{(1+\nu)}{(1-2\nu)}$ and hence, that of ν is controlled by $\frac{\partial G_\infty}{\partial T}$. Therefore, the composition dependence of the observed increase in ν above $T_g$ is simply a reflection of the behavior of $G_\infty(T)$.

## 4. Summary

The temperature dependence of the elastic moduli of $Ge_xSe_{100-x}$ glasses and deeply supercooled liquids with a range of structural connectivity and fragility are measured across $T_g$. While the temperature dependence of $G_\infty(T)$ in the glassy state is relatively weak and can be ascribed to the thermal expansivity, above $T_g$ the rapid drop in $G_\infty$ is consistent with it being proportional to the energy barrier to viscous flow via the creation of local free volume. Correlated variation between the $m$ and $|\frac{\partial G_\infty}{\partial T}|$ of these GFLs at $T > T_g$ indicates a fundamental connection between their entropic and elastic properties. However, the nature of this entropy remains unclear. The composition dependence of $|\frac{\partial \nu}{\partial T}|$ of these GFLs at $T > T_g$ is also controlled by that of $\frac{\partial G_\infty}{\partial T}$, as in this temperature range $|\frac{\partial G_\infty}{\partial T}| >> |\frac{\partial B_\infty}{\partial T}|$.

## Acknowledgments

This work was supported by a grant from the National Science Foundation (NSF-DMR 1855176).

**References:**

[1] A. Cavagna, Supercooled Liquids for Pedestrians, Phys. Rep. 476 (2009) 51–124. https://doi.org/10.1016/j.physrep.2009.03.003.

[2] J.C. Dyre, Colloquium: The glass transition and elastic models of glass-forming liquids, Rev. Mod. Phys. 78 (2006) 953–972. https://doi.org/10.1103/RevModPhys.78.953.

[3] G. Adam, J.H. Gibbs, On the Temperature Dependence of Cooperative Relaxation Properties in Glass-Forming Liquids, J. Chem. Phys. 43 (1965) 139–146. https://doi.org/10.1063/1.1696442.

[4] R.P. White, J.E.G. Lipson, Polymer Free Volume and Its Connection to the Glass Transition, Macromolecules. 49 (2016) 3987–4007. https://doi.org/10.1021/acs.macromol.6b00215.

[5] S. V. Nemilov, Structural aspect of possible interrelation between fragility (length) of glass forming melts and Poisson's ratio of glasses, J. Non. Cryst. Solids. 353 (2007) 4613–4632. https://doi.org/10.1016/j.jnoncrysol.2007.08.045.

[6] V. Lubchenko, P.G. Wolynes, Theory of Structural Glasses and Supercooled Liquids, Annu. Rev. Phys. Chem. 58 (2007) 235–266. https://doi.org/10.1146/annurev.physchem.58.032806.104653.

[7] S. Sen, Entropic vs. elastic models of fragility of glass-forming liquids: Two sides of the same coin, J. Chem. Phys. 137 (2012). https://doi.org/10.1063/1.4759155.

[8] W. Zhu, B. Aitken, S. Sen, Investigation of the Shear Relaxation Behavior of As-Se Liquids Within the Framework of Entropic and Elastic Models of Viscous Flow, J. Non. Cryst. Solids. 534 (2020) 119959. https://doi.org/10.1016/j.jnoncrysol.2020.119959.

[9] T. Rouxel, Thermodynamics of viscous flow and elasticity of glass forming liquids in the

glass transition range, J. Chem. Phys. 135 (2011). https://doi.org/10.1063/1.3656695.

[10] J.C. Dyre, T. Christensen, N.B. Olsen, Elastic Models for the Non-Arrhenius Viscosity of Glass-Forming Liquids, J. Non. Cryst. Solids. 352 (2006) 4635–4642. https://doi.org/10.1016/j.jnoncrysol.2006.02.173.

[11] C. A. Angell, Relaxation in Liquids, Polymers and Plastic Crystals - Strong/Fragile Patterns and Problems, J. Non. Cryst. Solids. 131 (1991) 13–31.

[12] D.L. Sidebottom, Fragility of network-forming glasses: A universal dependence on the topological connectivity, Phys. Rev. E. 92 (2015) 062804. https://doi.org/10.1103/PhysRevE.92.062804.

[13] R. Böhmer, K. L. Ngai, C. A. Angell, and D. J. Plazek, J. Chem. Phys. 99, 4201 (1993).

[14] F.F. Balakirev, S.M. Ennaceur, R.J. Migliori, B. Maiorov, and A. Migliori, Rev. Sci. Instrum. **90**, 121401 (2019).

[15] A. Migliori, J.L. Sarrao, W.M. Visscher, T.M. Bell, M. Lei, Z. Fisk, R.G. Leisure, Physica B **183**, 1 (1993).

[16] Y. Gueguen, T. Rouxel, P. Gadaud, C. Bernard, V. Keryvin, J.C. Sangleboeuf, High-Temperature Elasticity and Viscosity of $Ge_x Se_{1-x}$ Glasses in the Transition Range, Phys. Rev. B - Condens. Matter Mater. Phys. 84 (2011) 1–10. https://doi.org/10.1103/PhysRevB.84.064201.

[17] Y. Xia, B. Yuan, O. Gulbiten, B. Aitken, S. Sen, Kinetic and Calorimetric Fragility of Chalcogenide Glass-Forming Liquids: Role of Shear vs Enthalpy Relaxation, J. Phys. Chem. B. 125 (2021) 2754–2760. https://doi.org/10.1021/acs.jpcb.0c11278.

[18] E. Le Bourhis, Glass: Mechanics and Technology, in: Glas. Mech. Technol., 2007: pp. 271–274. https://doi.org/10.1002/9783527617029.app3.

[19] U. Senapati, A.K. Varshneya, Configurational Arrangements in Chalcogenide glasses: A new Perspective on Phillips' Constraint Theory, J. Non. Cryst. Solids. 185 (1995) 289–296. https://doi.org/10.1016/0022-3093(94)00534-6.

[20] J.C. Mauro, Y. Yue, A.J. Ellison, P.K. Gupta, and D.C. Allan, Proc. Natl. Acad. Sci. **106**, 19780 (2009).

[21] G.N. Greaves, A.L. Greer, R.S. Lakes, T. Rouxel, Poisson's Ratio and Modern Materials, Nat. Mater. 10 (2011) 823–837. https://doi.org/10.1038/nmat3134.

[22] R.K. Kirby, B.D. Rothrock, Thermal Expansion of Vitreous Selenium from—190° to +30°C, J. Am. Ceram. Soc. 51 (1968) 535–535. https://doi.org/10.1111/j.1151-2916.1968.tb15685.x.

[23] D.S. Sanditov, B.S. Sydykov, Modulus of Elasticity and Thermal Expansion Coefficient of Glassy Solids, Phys. Solid State. 56 (2014) 1006–1008. https://doi.org/10.1134/S1063783414050242.

[24] P. Koštál, J. Málek, Viscosity of selenium melt, J. Non. Cryst. Solids. 356 (2010) 2803–2806. https://doi.org/10.1016/j.jnoncrysol.2010.09.032.

[25] P. Koštál, J. Shánělová, J. Málek, Viscosity of Chalcogenide Glass-Formers, Int. Mater. Rev. 65 (2019) 63–101. https://doi.org/10.1080/09506608.2018.1564545.

[26] S.V. Nemilov, Viscosity and structure of Se-Ge Glasses., J. Appl. Chem. 37 (1964) 1020–1024.

**Figure Captions**

Fig. 1. A representative RUS scan (black line) of amorphous Se at 293K. Red crosses show the location of resonance peaks computed by the data acquisition code.

Fig. 2. Temperature dependence of $G_\infty$ of $Ge_xSe_{100-x}$ glasses and deeply supercooled liquids. Solid lines through the datapoints are guides to the eye. Arrows mark the break in slope corresponding to glass transition.

Fig. 3. Composition dependence of calorimetric (open squares) and elastic (filled squares) glass transition temperatures of $Ge_xSe_{100-x}$ glasses.

Fig. 4. $|\frac{\partial G_\infty}{\partial T}|$ of $Ge_xSe_{100-x}$ glasses measured in the present study as a function of their thermal expansion coefficient as reported in the literature [19,22,23].

Fig. 5. Viscosity of $Ge_xSe_{100-x}$ supercooled liquids as a function of $T_g/T$ (open symbols) and $G_\infty(T)/T$ (filled symbols). Here $G_\infty/T$ is also normalized to 1 at T = $T_g$ for ease of comparison. Viscosity [24–26] data are taken from the literature. Solid line through the filled symbols is a linear least squares fit to the data.

Fig. 6a. $|\frac{\partial G_\infty}{\partial T}|$ of supercooled $Ge_xSe_{100-x}$ liquids measured in the present study as a function of their fragility index $m$ obtained from viscosity data reported in the literature [24–26].

Fig. 6b. Parameter $\frac{1}{1-\chi}$ (see text for details) as a function of fragility index $m$ of supercooled $Ge_xSe_{100-x}$ liquids obtained from viscosity data reported in the literature [24–26].

Fig. 7. Temperature dependence of Poisson's ratio ν of $Ge_xSe_{100-x}$ glasses and deeply supercooled liquids. Solid lines through the datapoints are guides to the eye.

Fig. 8. Temperature dependence of $B_\infty$ and of $G_\infty$ of supercooled $Ge_xSe_{100-x}$ liquids at T > $T_g$.

**Figure 1**

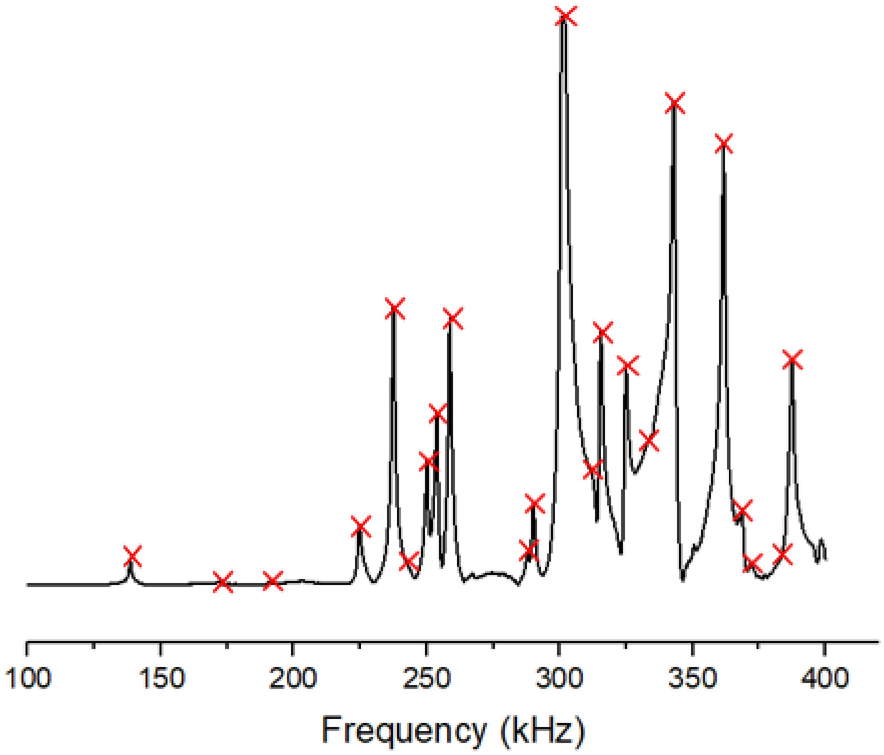

**Figure 2**

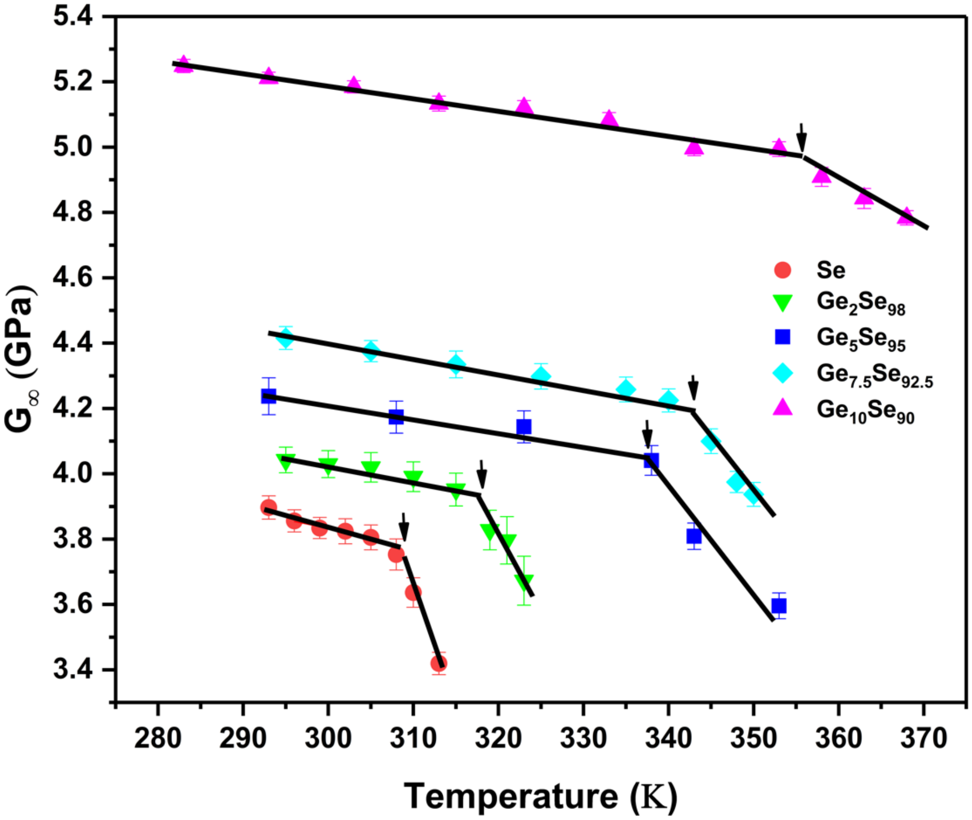
$G_\infty$ (GPa)
Temperature (K)
5.4
5.2
5.0
4.8
4.6
4.4
4.2
4.0
3.8
3.6
3.4
280
290
300
310
320
330
340
350
360
370
Se
$Ge_2Se_{98}$
$Ge_5Se_{95}$
$Ge_{7.5}Se_{92.5}$
$Ge_{10}Se_{90}$

**Figure 3**

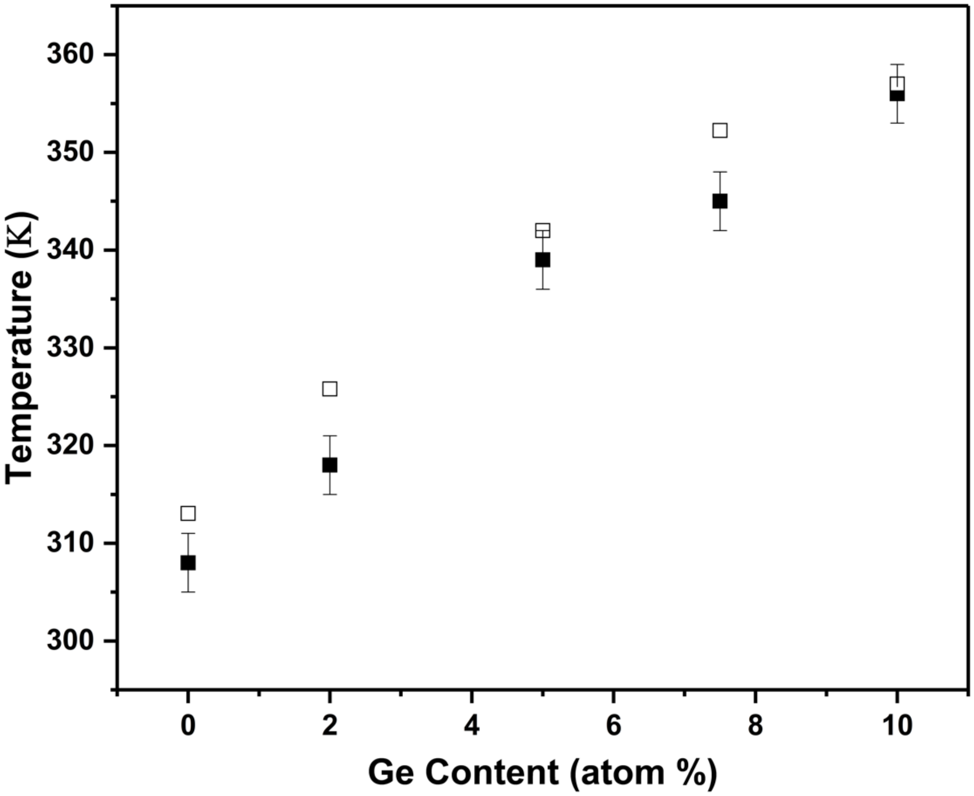
Temperature (K)
300
310
320
330
340
350
360
0
2
4
6
8
10
Ge Content (atom %)

**Figure 4**

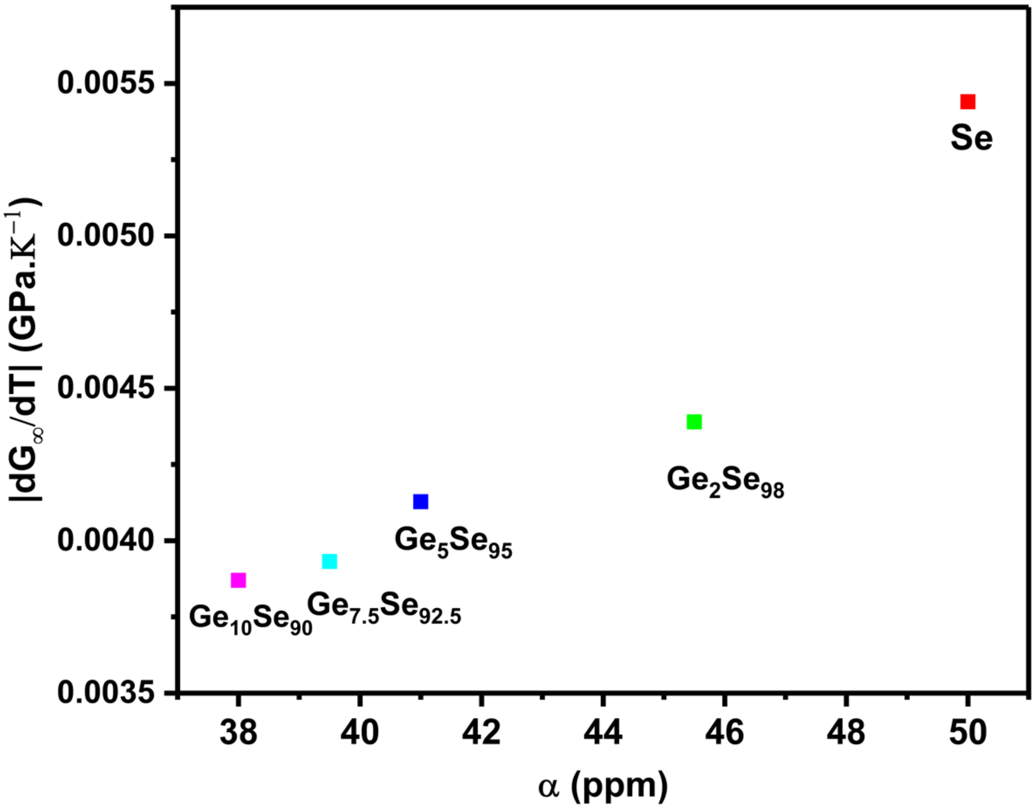
|dG$_\infty$/dT| (GPa.K$^{-1}$)
0.0055
0.0050
0.0045
0.0040
0.0035
α (ppm)
38
40
42
44
46
48
50
Se
Ge$_2$Se$_{98}$
Ge$_5$Se$_{95}$
Ge$_{10}$Se$_{90}$
Ge$_{7.5}$Se$_{92.5}$

**Figure 5**

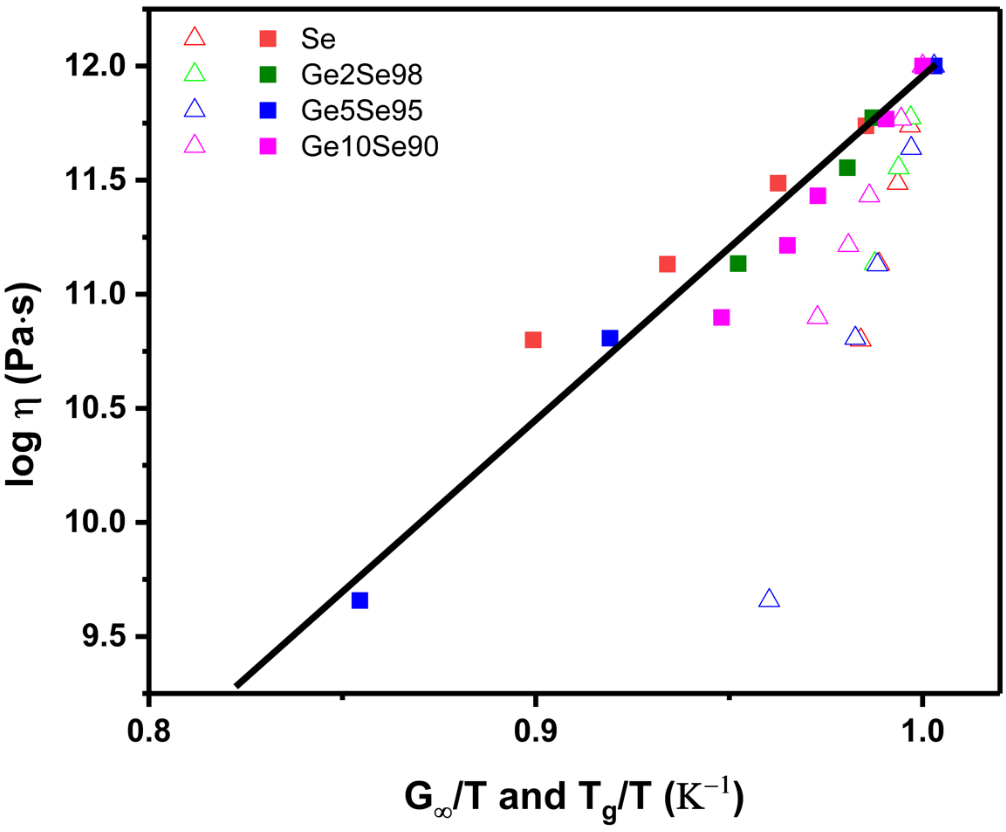

△ ■ Se
△ ■ Ge2Se98
△ ■ Ge5Se95
△ ■ Ge10Se90
log η (Pa·s)
12.0
11.5
11.0
10.5
10.0
9.5
0.8
0.9
1.0
$G_\infty/T$ and $T_g/T$ ($K^{-1}$)

**Figure 6a**

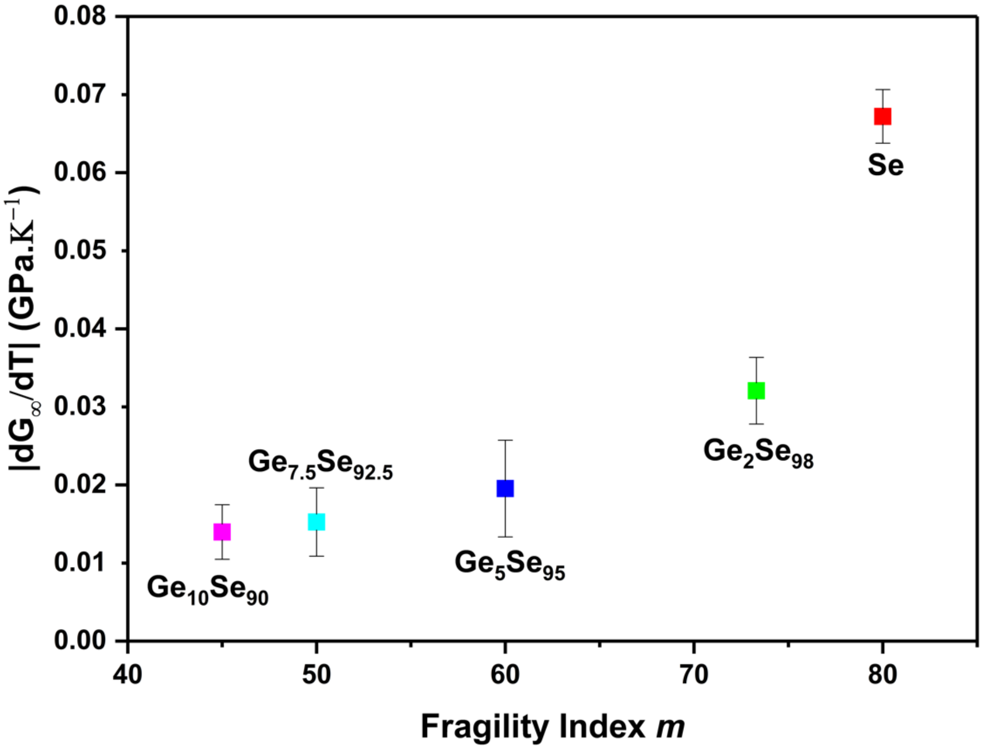
$|dG_\infty/dT|$ (GPa.K$^{-1}$)
0.00
0.01
0.02
0.03
0.04
0.05
0.06
0.07
0.08
Fragility Index *m*
40
50
60
70
80
Se
$Ge_2Se_{98}$
$Ge_{7.5}Se_{92.5}$
$Ge_5Se_{95}$
$Ge_{10}Se_{90}$

**Figure 6b**

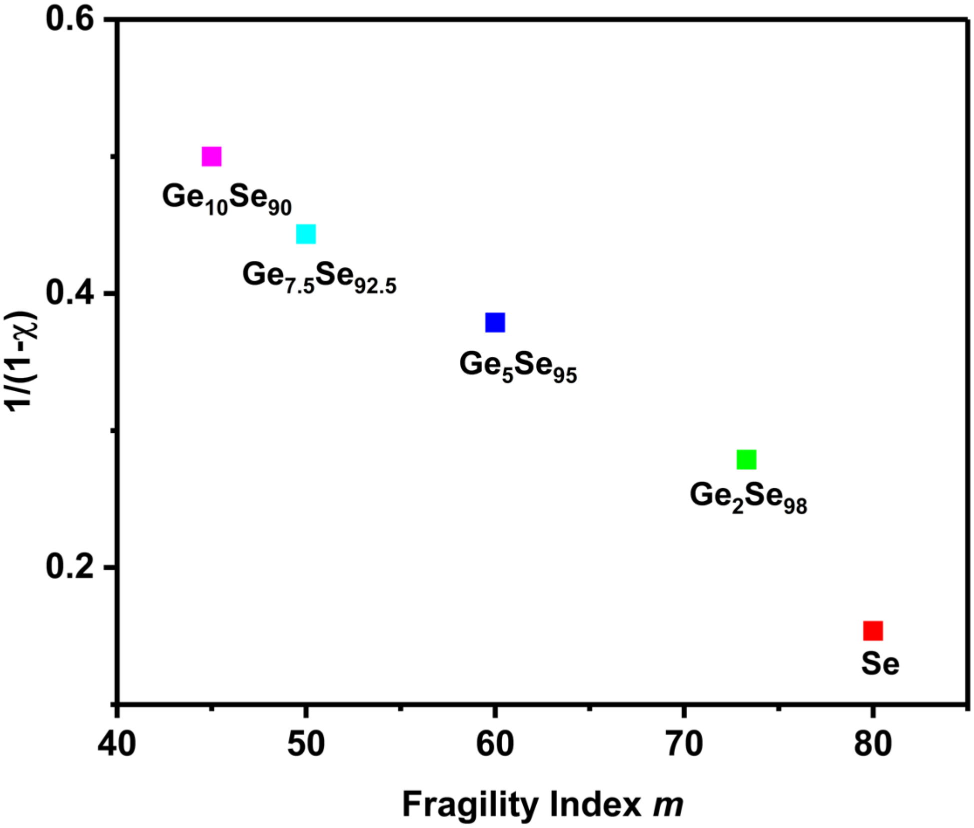
0.6
0.4
0.2
1/(1-χ)
40
50
60
70
80
Fragility Index m
Ge10Se90
Ge7.5Se92.5
Ge5Se95
Ge2Se98
Se

**Figure 7**

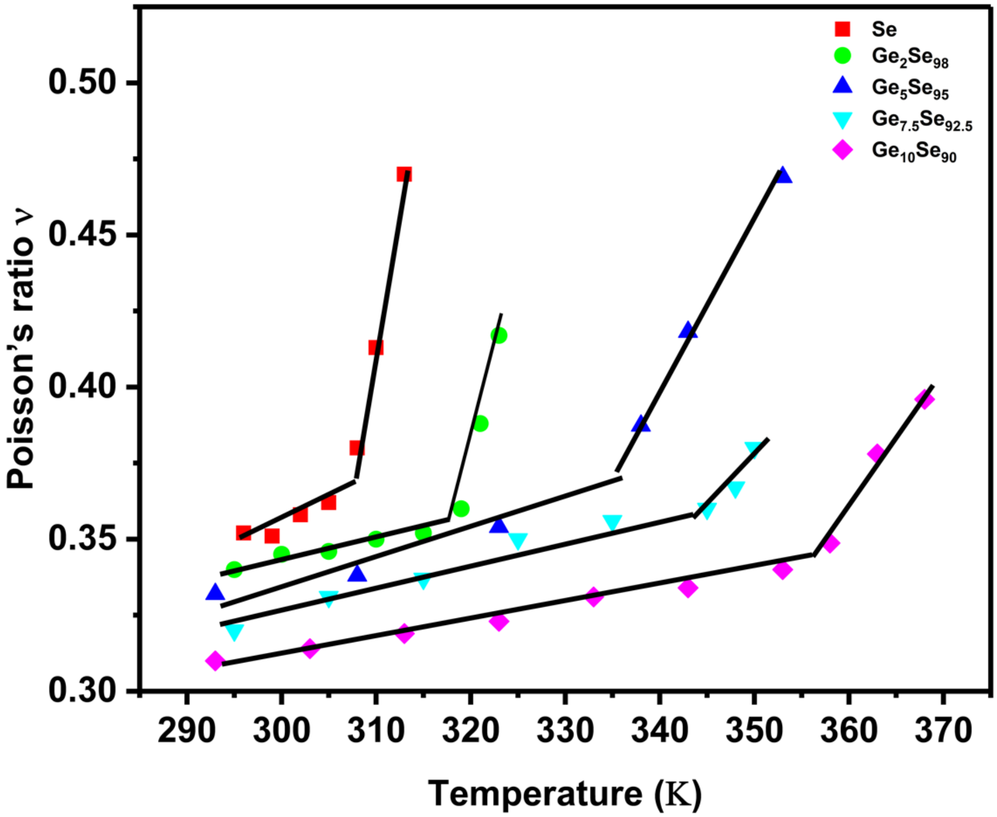

Se
$Ge_2Se_{98}$
$Ge_5Se_{95}$
$Ge_{7.5}Se_{92.5}$
$Ge_{10}Se_{90}$
Poisson's ratio ν
0.50
0.45
0.40
0.35
0.30
290
300
310
320
330
340
350
360
370
Temperature (K)

**Figure 8**

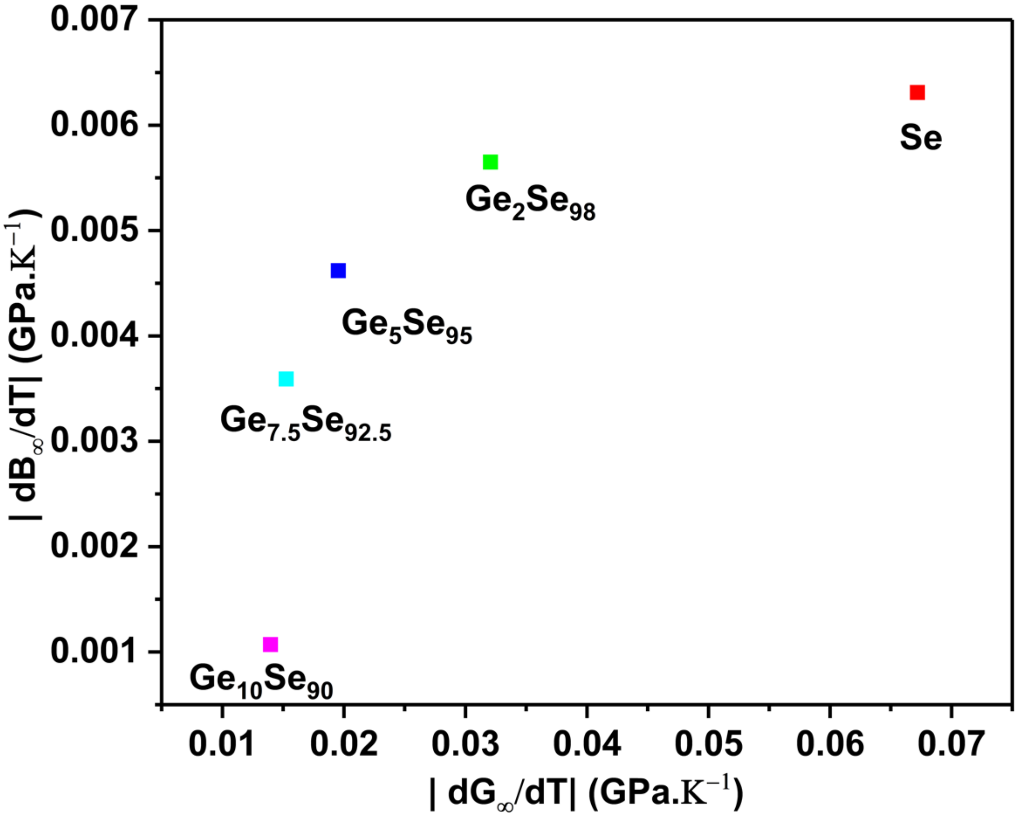
0.007
0.006
0.005
0.004
0.003
0.002
0.001
| dB$_\infty$/dT| (GPa.K$^{-1}$)
0.01
0.02
0.03
0.04
0.05
0.06
0.07
| dG$_\infty$/dT| (GPa.K$^{-1}$)
Se
$Ge_2Se_{98}$
$Ge_5Se_{95}$
$Ge_{7.5}Se_{92.5}$
$Ge_{10}Se_{90}$